A Frequency and Polarization Reconfigurable Transparent Water Antenna

Lei Li[1, 2, *], Jing Gao[1, 2], and Jingchang Nan[1, 2]

[1]*School of Electronics and Information Engineering, Liaoning Technical University, Huludao 125105, China*
[2]*Liaoning Key Laboratory of Radio Frequency and Big Data for Intelligent Applications, Huludao 125105, China*

ABSTRACT: A novel frequency and polarization reconfigurable water patch antenna is proposed for radio communication in the UHF band. Based on theoretical analysis and simulation results, water is an ideal material for designing transparent liquid ground. Water enhances outstanding transparency, excellent aesthetics, and high optical stealth performance for a wider range of application scenarios. The entire structure is made with polyvinyl chloride material and distilled water, except for the feed structure. By filling different cavities with liquid water, five different operating states are obtained in 1.924–2.5 GHz (26.1%), 1.67–2.33 GHz (33%), 0.644–2.288 GHz (112.1%), 1.975–2.54 GHz (25%), and 1.748–2.108 GHz (18.7%), achieving frequency reconfigurability. The antenna can be flexibly switched between linear polarization (LP) and two right-handed circular polarization (RHCP) states. The results show that the 3 dB axial ratio (AR) bandwidth covers 1.93–2.08 GHz (7.5%) and 2.06–2.132 GHz (3.5%). The antenna achieves high optical transparency of 100% and a peak gain of 7.97 dBi.

1. INTRODUCTION

Reconfigurable antennas can dynamically change the impedance and radiation characteristics through the actual working environment and realize the functions of multiple antennas through a single antenna [1, 2]. The antennas are extensively utilized due to their light weight, miniaturization, and low cost. Conventional reconfigurable antennas usually employ electrical switches to change the structure and size of the antenna [3–5] to achieve flexible switching between different states. However, the additional power source leads to nonlinear distortion, limiting their application to high-power radio frequency (RF) conditions.

Recent years have witnessed a tremendous interest toward developing frequency and polarization reconfigurable antennas with high fluidity of liquid materials. Compared with electrically controlled reconfigurable antennas, liquid antennas have the advantages of continuous tunability, wide tunable range, and high radiation efficiency. Moreover, its functional versatility can be realized by conveniently pumping in or out the liquid without changing the structure, significantly mitigating the nonlinear distortion caused by electrical switches. Numerous liquid antennas have been reported, such as monopole antennas, dielectric resonator antenna (DRA), and patch antennas [6–8]. In [9], a new pure water inverted L antenna is proposed. The frequency reconfigurability of the antenna is achieved by changing its cross-section. The operating band of the water antenna can be tuned from 1.41–2.04 GHz to 1.07–1.33 GHz. In [10], a circularly polarized reconfigurable patch antenna is proposed by injecting liquid dielectric into different channels in the substrate. The antenna can be switched between left-

handed circular polarization (LHCP) and right-handed circular polarization (RHCP). A stable circularly polarized gain of 8 dBi and 90% efficiency in 2.24–2.52 GHz are achieved. In [11], a polarization and frequency reconfigurable liquid antenna is proposed. The antenna can be flexibly switched between linear and dual circular polarizations by changing the liquid injection position and obtaining four reconfigurable frequency bands. It has a 42% frequency adjustable range, and peak gain reaches 5.07 dBi.

Owing to the fluidity and high transparency of liquids, the design of transparent antennas using liquid has become a novel idea in the current field of reconfigurable antenna design. Transparent antennas can be perfectly integrated into various transparent structures or equipment, such as glass curtain walls. Their hidden design fulfills the requirement of modern buildings and equipment for aesthetic appearance, harmonizing the antenna with the surrounding environment. Transparent materials are the key to building transparent antennas, and the most commonly used materials are transparent conductive oxide (TCO) [12] and transparent conductive film (TCF) [13]. The two materials have both transparency and conductivity, but they are expensive to manufacture and not easily available. Mesh metal layers [14] offer another method of creating transparent antennas. It is common practice to etch periodic holes or gaps on the metal patch and ground. However, it does not provide both better radiation efficiency and optical transparency. All three of these transparent antennas utilize a metal ground, which greatly reduces the overall optical transparency of the antenna. Liquid water is an inexpensive and readily available material with 100% optical transparency that can be used to make transparent ground [15, 16]. In 2017, a water patch antenna was first proposed, and both the patch and the ground
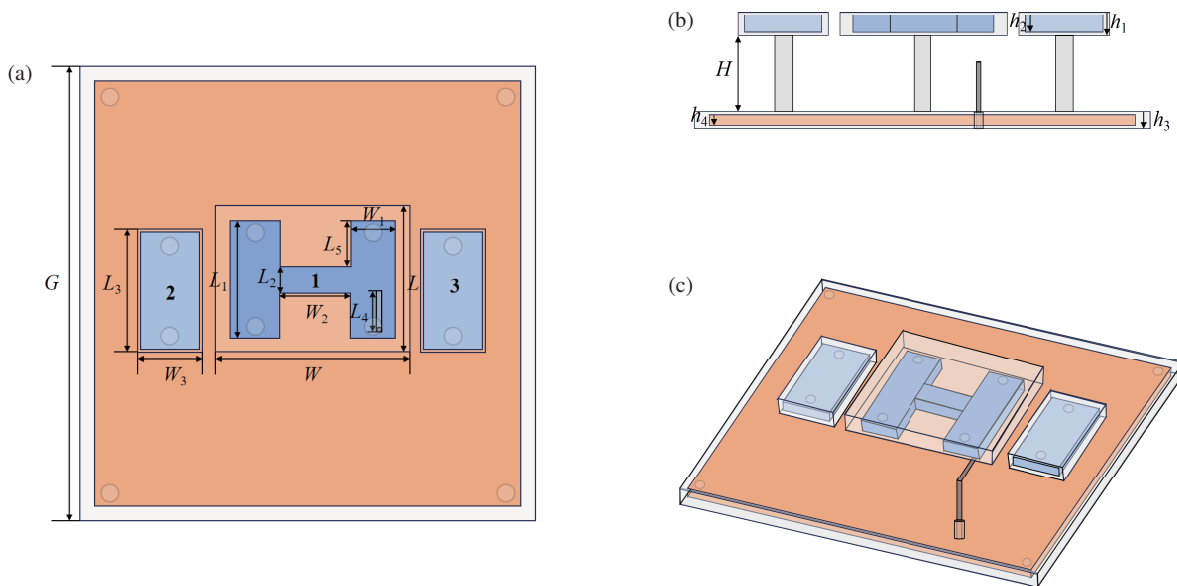
FIGURE 1. Detailed geometry of the proposed antenna. (a) Top view. (b) Side view. (c) 3D view.

TABLE 1. Antenna optimized parameter values.

Parameters	Value/mm	Parameters	Value/mm	Parameters	Value/mm
G	155	L	50	L_5	9
W	66	L_1	40	H	18
W_1	16	L_2	15.5	h_1	7.8
W_2	24	L_3	42	h_2	5.8
W_3	22	L_4	14	h_3	5.5

were composed of distilled water [17]. In the operating band of 2.0–2.85 GHz, a relative bandwidth of 35% and a gain up to 4.0 dBi were achieved. In [18], a proposed fully transparent water antenna with an impedance bandwidth of 29% achieved a gain of 3.05 dBi and a maximum radiation efficiency of 48% of the operating band. It has been demonstrated that water offers significant performance and transparency benefits over other materials for transparent antennas, which has great potential in constructing transparent antennas.

In this paper, a frequency and polarization reconfigurable water patch antenna with high optical transparency is proposed. The difference in reflection coefficient performance when liquid ground is designed using different liquids is discussed. The performance of the antenna is compared when different liquids and metals are used as ground design materials. The results demonstrate the greater advantage of water as a transparent antenna material. Both the patch and the ground are composed of polyvinyl chloride material and distilled water to provide great optical transparency at a minimal cost. The final design of the antenna can be switched between LP and two RHCP states. Meanwhile, the antenna has frequency reconfigurable performance between 0.64 and 2.54 GHz. In addition, the effects of using a Γ-shaped probe, water patch thickness, and air substrate thickness on antenna performance are discussed.

2. ANTENNA DESIGN

2.1. Antenna Geometry

The geometry of the proposed water patch antenna is depicted in Fig. 1. The structure consists of an H-shaped main water patch, two parasitic water patches, a water ground, and a Γ-shaped feed probe. The water patches are above the water ground, and an air layer is in the middle.

Distilled water is a liquid material with high transparency and dielectric constant. It has ε_r and $\tan(\delta)$ of 81.0 and 0.008, respectively. Distilled water is contained in a high-transparency polyvinyl chloride container to ensure excellent optical transparency of the antenna.

Using the Γ-shaped probe as a feed structure, to ensure that all electromagnetic (EM) waves are transmitted into the air, the inner conductor of the SMA must completely penetrate the through-hole of the liquid ground. The inner conductor of the SMA is directly connected to the metal probe, and the outer conductor is encircled by the water ground.

The main dimensions of the antenna are shown in Table 1.

2.2. Realization of Transparency

The overall transparency of the antenna structure can be greatly improved by using transparent water ground in place of the

TABLE 2. Reflection coefficient.

θ / Material	0°	15°	30°	45°	60°
Metal Ground	$\Gamma_v = 0.52$	$\Gamma_v = 0.51$	$\Gamma_v = 0.47$	$\Gamma_v = 0.39$	$\Gamma_v = 0.24$
Water Ground	$\Gamma_v = 0.80$	$\Gamma_v = 0.79$	$\Gamma_v = 0.77$	$\Gamma_v = 0.73$	$\Gamma_v = 0.64$
TPC Ground	$\Gamma_v = 0.30$	$\Gamma_v = 0.29$	$\Gamma_v = 0.25$	$\Gamma_v = 0.17$	$\Gamma_v = 0.02$
EA Ground	$\Gamma_v = 0.42$	$\Gamma_v = 0.41$	$\Gamma_v = 0.36$	$\Gamma_v = 0.29$	$\Gamma_v = 0.13$
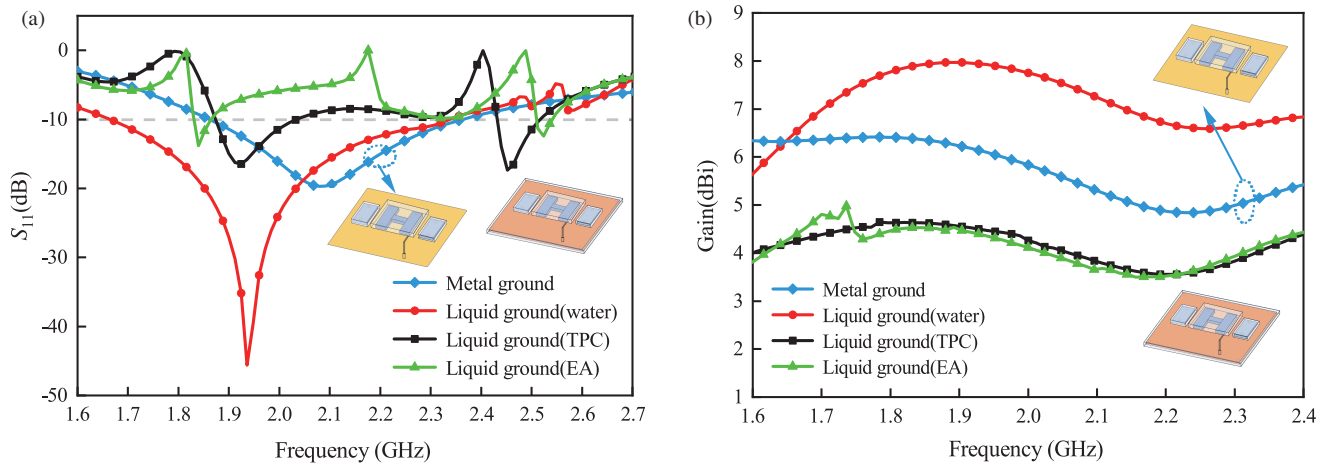
FIGURE 2. Comparison of simulation results of antennas with metal ground and liquid ground. (a) S_{11}. (b) Gain.

metal ground in antennas. Since the relative permittivity of water is much larger than air, the water patch can closely resemble a metallic electric wall. EM waves are bound between the upper water patch and the water ground, limiting the propagation of EM waves in the air layer. This phenomenon can be explained through the formulas as follows [19].

For equations,

$$\varepsilon = \varepsilon_r - j18 \times 10^3 \frac{\sigma}{f_{MHz}} \qquad (1)$$

$$\Gamma_v = \frac{\varepsilon \cos \theta - \sqrt{\varepsilon - \sin^2 \theta}}{\varepsilon \cos \theta + \sqrt{\varepsilon - \sin^2 \theta}} \qquad (2)$$

$$T \approx T_c \times T_w \qquad (3)$$

In (1), ε_r is the relative dielectric constant, and σ is the conductivity. When σ is very small and the frequency very high, the imaginary part of formula can be neglected, and ε_r will become the dominant value of ε. Therefore, the imaginary part of the non-ideal ground plane can be neglected when the reflection coefficient is calculated. In (2), θ is the reflection angle of an incident plane wave when the antenna is placed on a non-ideal ground. In (3), T is the transparency of the antenna, T_c the transmission of the container, and T_w the transmission of the water patch.

The ε_r of metal ground, water, trihexyltetradecylphosphonium chloride (TPC), and ethyl acetate (EA) are taken as 10, 81, 3.4, and 6, respectively. The reflection coefficients of these materials can be calculated according to (2), and the specific

comparison results are shown in Table 2. It can be seen that distilled water has a better reflection coefficient and can reflect electromagnetic energy better, which can be used as a better choice for liquid ground design.

To verify the reasonableness of the above analysis, the antenna performance on the metal ground and different liquid grounds were simulated. The simulation results are shown in Fig. 2. From the antenna comparison, it can be seen that the water and metal ground antennas have wider impedance bandwidth and higher gain. Since metal is an opaque material, this antenna can only achieve transparency of the patch structure, reducing the overall transparency of the antenna. Antennas using water ground have better relative bandwidth and gain than antennas using other liquid ground. Due to its high dielectric constant, water reflects EM waves better than other materials. This is consistent with the analytical conclusions of the computational results of (2).

Furthermore, the selected liquid must be colorless and transparent to fulfill the design requirements for a transparent liquid ground. Water has higher transparency, more stable chemical properties, and lower viscosity than the majority of transparent ionic liquids or organic solvents. These advantages of water are beneficial to designing transparent antennas and improving reconfigurable efficiency. Therefore, water ground may be a better choice for the design of transparent antennas. Based on the transparency specification data of transparent packaging materials, under ideal conditions where the container is completely transparent ($T_c = 1$) and the purity of water extremely
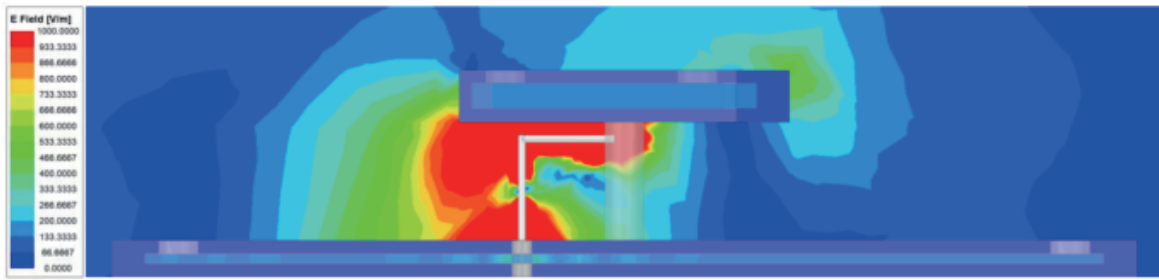
FIGURE 3. Magnitude distributions of the electric field at 1.936 GHz.

high (considered to have a transmittance of 100%, $T_w \approx 1$), we conclude that the transparency of the designed water patch antenna is close to 100%.

3. WORKING PRINCIPLE

The water patch antenna takes advantage of the electric wall-like effect at the interface between water with a high dielectric constant and air with a low dielectric constant to replace the conventional metal patch. The electromagnetic wave is bound between the water patch and water ground to make it radiate outward from the gap. Due to the large difference between the dielectric constants of water and air, when the EM wave is reflected from the water medium to the air, total reflection occurs at the interface, similar to the reflection of electromagnetic waves on an electric wall. This total reflection effect makes the water patch equivalent to an electric wall in terms of electromagnetic properties. The magnitude distributions of the electric field in the E-plane at 1.936 GHz are shown in Fig. 3. It is further demonstrated that there is almost no current inside the distilled water, and the water patch serves only to establish boundary conditions similar to an electric wall, where the electric field generated by the Γ-probe exists primarily in the air substrate.

The electromagnetic wave would ideally radiate uniformly in all directions for a water patch fed at the center. When this plane wave has an electric field along the vertical direction, it excites the electrons on the surface of the water patch to move in the vertical direction, as shown in Fig. 4(a). A current (i_y) is generated in the vertical direction. Due to the symmetry of the antenna structure, the impedance is symmetrical in the horizontal direction. Thus, the currents in the horizontal direction (i_x) are equal in magnitude, opposite in direction, and canceled.
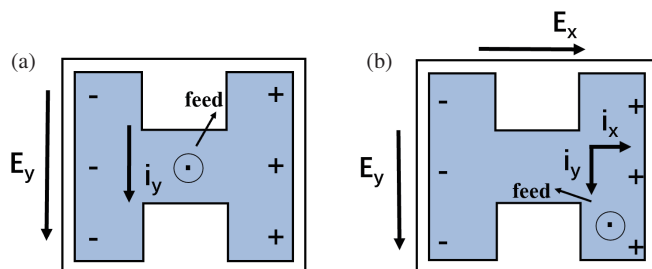
However, when the feed point is off-center, the electric field in the vertical direction is incident on the surface of the water patch. As shown in Fig. 4(b), it still causes the electrons to move along the vertical direction, generating i_y. At the same time, the current path is changed when the structure is not symmetrical. The inhomogeneous surface impedance in the horizontal direction will be introduced. Then, a potential difference and a current are generated, resulting in an electric field in the horizontal direction (E_x). E_x and E_y are orthogonal to each other.

By adjusting the position and size of the feed probe, E_x and E_y are equal in amplitude and have a 90° phase difference at 2.07 GHz. As a result, two linearly polarized waves with the same amplitude and a 90° phase difference are formed, and circular polarization is finally obtained. The E-field vector distributions of the water patch at 2.07 GHz frequency with different phases are shown in Fig. 5. In states 1 and 2, when the current rotates counterclockwise, the antenna can achieve right-handed circular polarization.

The radiation patterns at 2.07 GHz are shown in Fig. 6. It demonstrates that co-polarization is RHCP, while LHCP is cross-polarization. In the maximum radiation direction, the RHCP exceeds the LHCP by more than 15 dB. The patterns have larger back radiation, although theoretical calculations indicate that the reflection performance of a water ground is superior to that of a metal ground. In actual experiments, due to disadvantages in packaging materials, thin or uneven water layers, and other factors, some EM waves can still pass through the water ground and radiate backward, resulting in higher back radiation. It can be seen that the simulated results are very similar to the measured ones, although there are some differences. This error may be caused by the presence of irregular PVC residues during the fabrication of the physical cavity.

4. PERFORMANCE

In this work, a prototype sample is fabricated and measured to validate the above design ideas. Fig. 7 depicts the 3D view and top view of the actual antenna. As shown, the antenna has great transparency performance.

To verify the simulation performance of the water patch antenna proposed in this paper, a liquid ground cavity, an H-shaped cavity, and two parasitic rectangular cavities are fabricated using 3D printing. Using a microfluidic pump, the frequency and polarization can be reconfigured quickly. As shown

FIGURE 4. Current distribution. (a) Fed at the center. (b) Feed point is off-center.
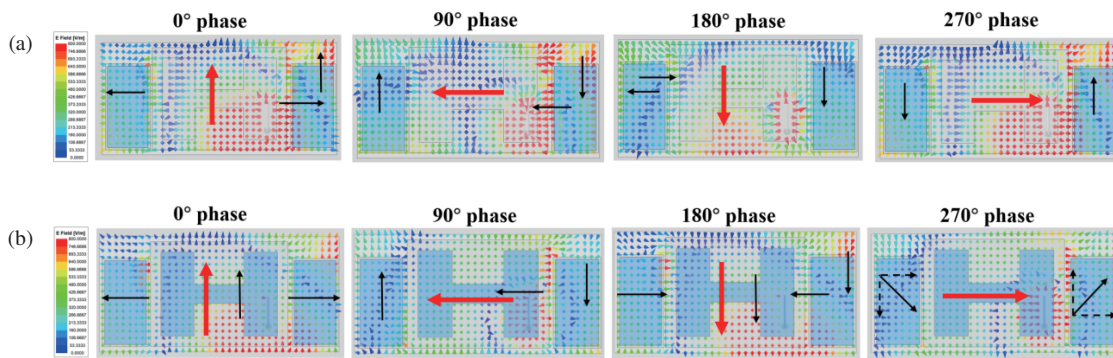
FIGURE 5. *E*-field vector distribution of the antenna in RHCP at different phases. (a) State 1. (b) State 2.
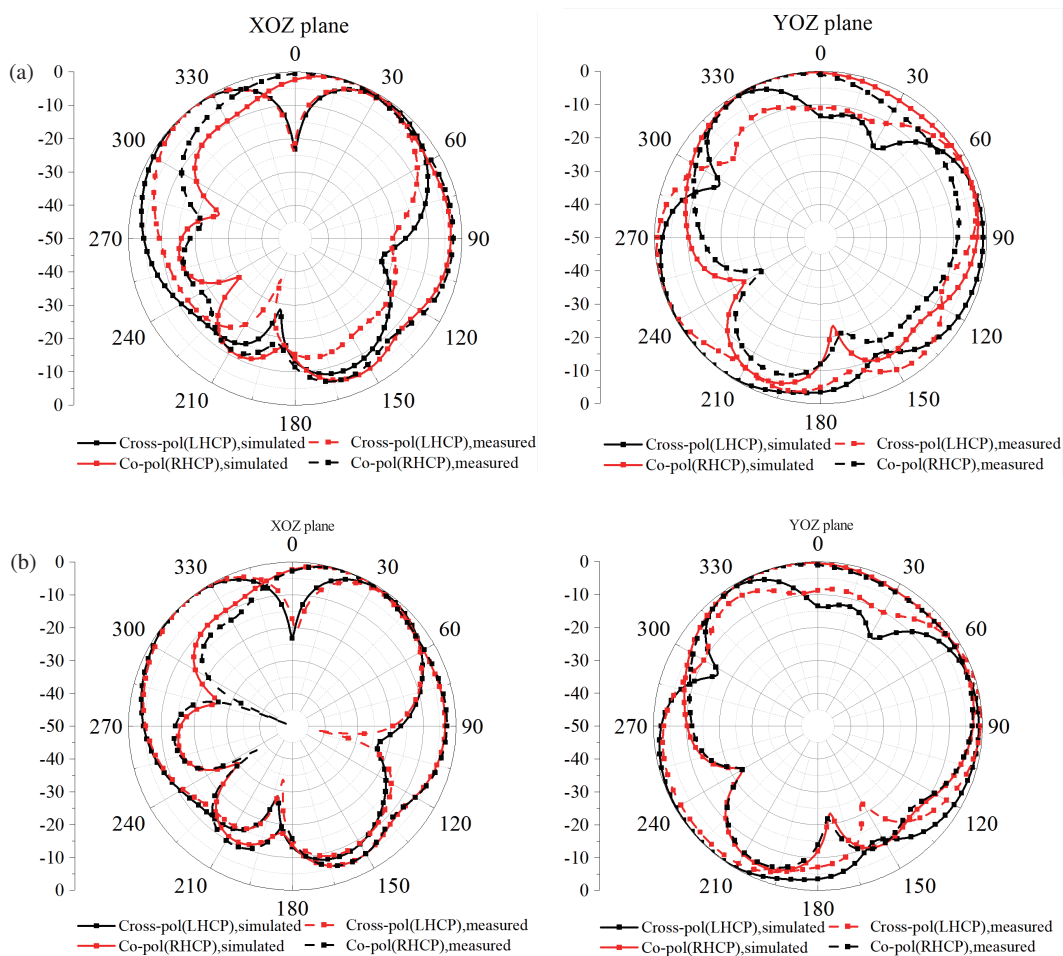
FIGURE 6. Simulated and measured radiation patterns. (a) State 1. (b) State 2.

in Fig. 8, the results show that there are two states of the antenna in RHCP. When cavities 2 and 3 (state 1) are filled with water, the measured impedance bandwidth is 1.924–2.5 GHz (26.1%). When the full cavity is filled with water (state 2), the measured impedance bandwidth can cover 1.67–2.33 GHz (33%), which is slightly wider than the simulation results. The antenna has three states in LP state. Only when cavity 2 (state 3) is filled with water, the measured impedance bandwidth is 0.644–2.288 GHz (112.1%), which is better than the simulation

results. When cavities 1 and 2 (state 4) are filled with water, the measured impedance bandwidth covers 1.975–2.54 GHz (25%). When only cavity 3 (state 5) is filled with water, the measured impedance bandwidth is 1.748–2.108 GHz (18.7%). Slight discrepancies between the measured and simulated values of the antenna are usually the result of errors in the manufacturing and testing process, but the measured and simulated values can still be matched. The simulated and measured operating frequencies of each state are shown in Table 3.
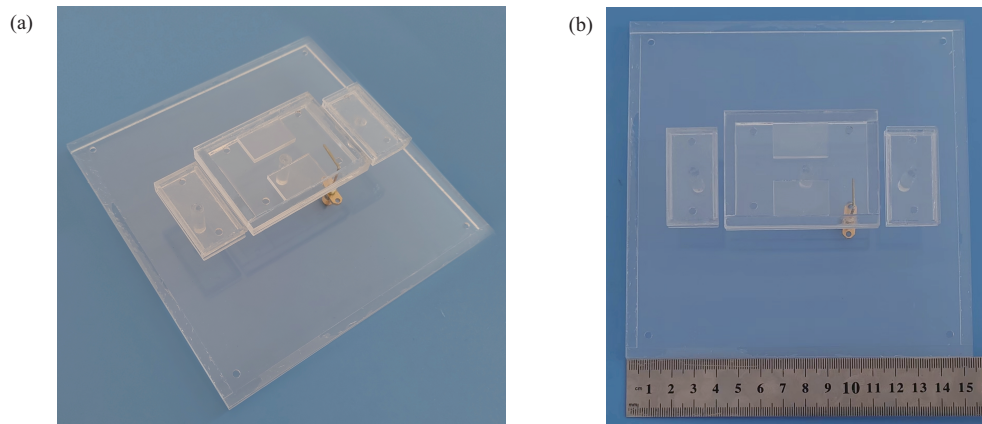
FIGURE 7. Prototype of the proposed antenna. (a) 3D view. (b) Top view.
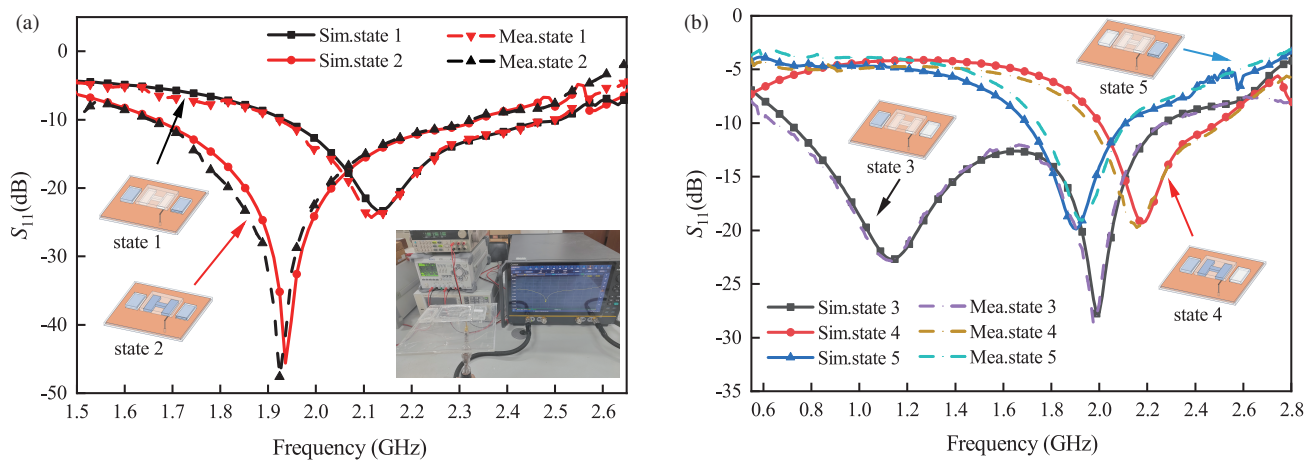
FIGURE 8. The simulated and measured S_{11} curves of the antenna in different reconfigurable states and the testing environment. (a) RHCP state. (b) LP state.

TABLE 3. Simulated and measured operating frequencies of each state.

State	Simulated operating frequency (GHz)	Measured operating frequency (GHz)
1	1.936–2.5	1.924–2.5
2	1.65–2.3	1.67–2.33
3	0.704–2.276	0.644–2.288
4	2.012–2.49	1.975–2.54
5	1.688–2.09	1.748–2.108

Figure 9 shows the simulated and measured curves of the 3 dB AR in RHCP. The measured bandwidth of the 3 dB AR for state 1 is 2.06–2.132 GHz (3.5%), and the measured bandwidth of the 3 dB AR for state 2 covers 1.928–2.08 GHz (7.6%). For RHCP, although the measured AR bandwidth of the antenna is slightly different from the AR bandwidth of the simulation results, the measured curves still have a similar trend to the simulation results. Fig. 10 shows the gain comparison of the water patch antenna in two states of RHCP. In state 1, the antenna has a minimum gain of 3.57 dBi and a maximum gain of 6.7 dBi. In state 2, the antenna has a minimum gain of 5.43 dBi and a maximum gain of 7.97 dBi. The maximum gain error is 0.75 dBi compared with the simulation results. It is mainly due to the

error in the dielectric constant of the PVC material and the differences generated in the fabrication process, which affect its radiation performance. The radiation patterns of states 3, 4, 5, and 6 are shown in Fig. 11.

5. DISCUSSION

The Γ-shaped metal probe feed structure is used in Fig. 1(c) to optimize the impedance matching and broaden the impedance bandwidth. 50 Ω coaxial cable is extended through the water ground plane to the middle substrate, and the Γ-shaped metal probe is coupled to the upper water patch. The inductive reactance is generated between the vertical part of the Γ-shaped
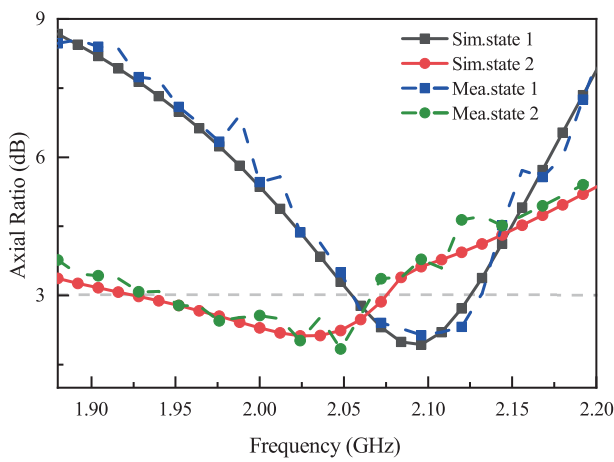
FIGURE 9. The simulated and measured AR curves of the antenna in RHCP state and fabricated prototype.
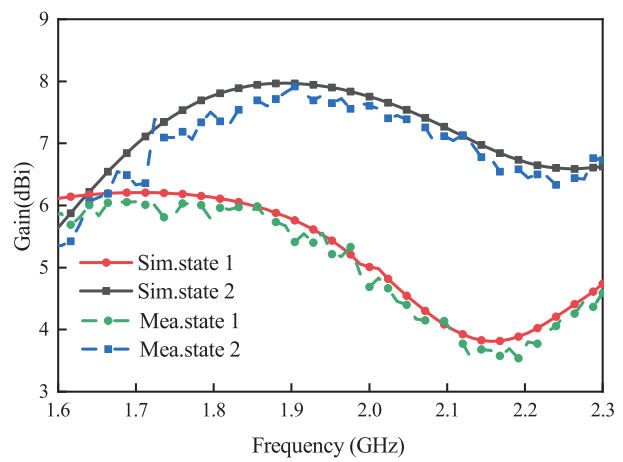
FIGURE 10. The simulated and measured realized gains of the antenna in RHCP state.
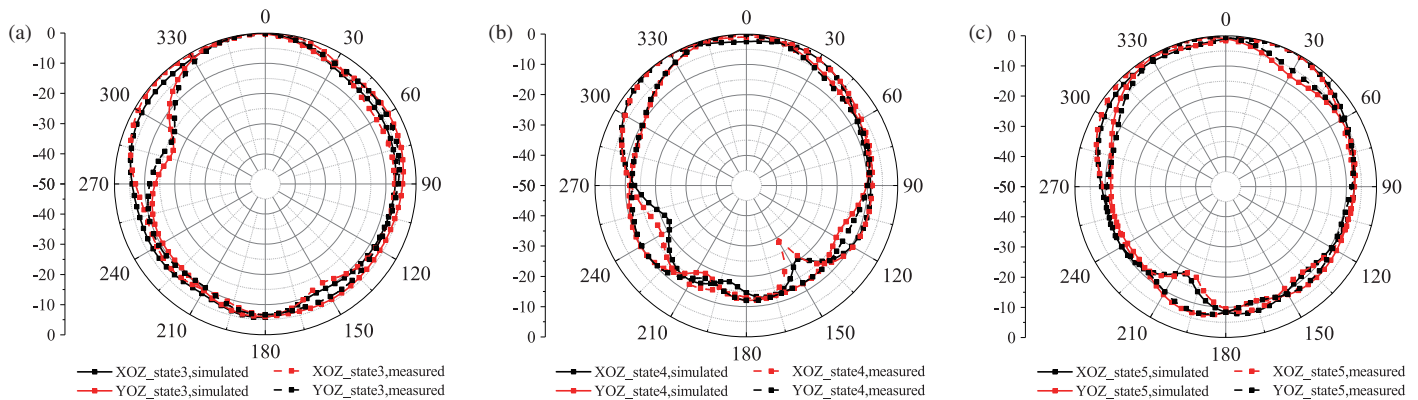
FIGURE 11. Simulated and measured radiation patterns. (a) State 3. (b) State 4. (c) State 5.

probe and the patch, and the capacitive reactance is generated between the horizontal part and the patch. The inductive and capacitive reactances interact to produce resonance so that the antenna frequency band is broadened. The radiation performance, radiation pattern, and 3D radiation pattern comparison between using an Γ-shaped metal probe and using a normal probe ($L_4 = 0$) are shown in Fig. 12. It turns out that when the proposed antenna is fed only by a vertical metal probe, it can also achieve almost the same radiation characteristics as that fed by a Γ-shaped water probe, indicating that the radiation is from the water patch rather than from the probe.

Two key parameters that distinguish the antenna from the conventional metal patch antenna are selected for study and discussion.

In the simulation, a metal patch usually has no thickness. However, the patch of water patch antenna has thickness. This thickness is simulated and studied. The AR bandwidth for different thicknesses of water patches is shown in Fig. 13. The center frequency of the AR bandwidth decreases from 2.25 GHz to 2.036 GHz while the thickness of the water patch grows from 3 mm to 5.8 mm. The resonant frequency decreases as the water patch thickness increases. This is because as the thickness of the water layer increases, the distribution of the electric field

inside the water patch becomes more intense, resulting in an increase in the effective electric height, as shown in Fig. 14, where the red area represents high electric field strength. As the thickness of the water layer increases, the red areas will significantly expand, indicating that the concentration of the electric field inside the water patch is increasing. This change in electric field distribution not only affects the effective electric height, but also further affects the equivalent capacitance and inductance. Due to the accumulation of more charges in a smaller space by the electric field, the equivalent capacitance increases. Meanwhile, the extension of the electric field inside the water patch also changes the equivalent inductance. These changes in capacitance and inductance collectively lead to a decrease in resonance frequency. Antennas now require lower frequencies to reach resonance because changes in electric field distribution have altered the conditions for resonance.

To investigate the impact of air layer height on antenna gain. The air substrate is simulated with different thicknesses, and the results are displayed in Fig. 15. It shows that the gain increases significantly along with the thickness of the substrate. As the thickness of the intermediate substrate increases from 12 mm to 21 mm, the gain improves from 7.16 dBi to 8.55 dBi. Because the two slots between the edges of the water patches and wa-
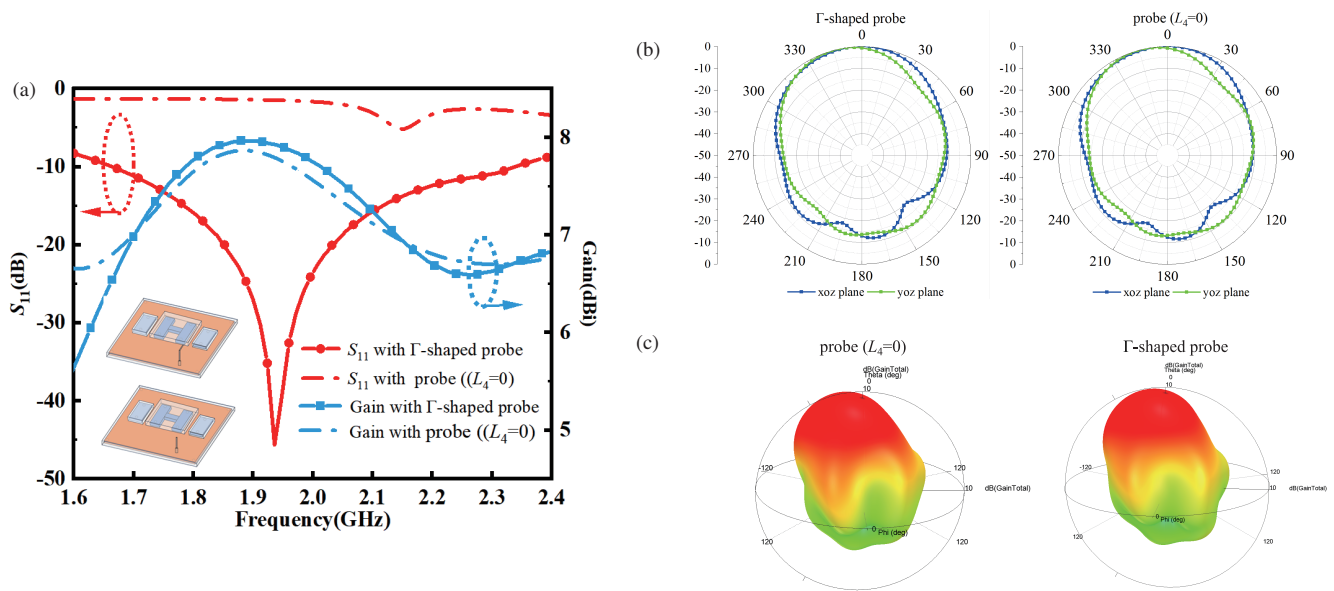
FIGURE 12. Simulated results: (a) S_{11} and gain. (b) Radiation patterns at 1.936 GHz. (c) 3D radiation patterns.
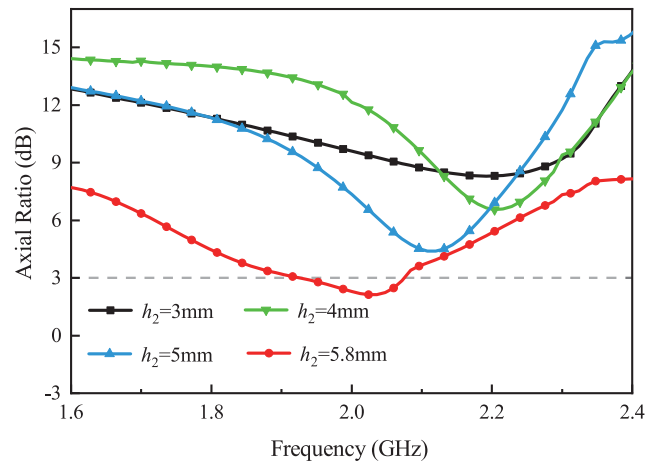
FIGURE 13. Simulated AR bandwidths with different thicknesses of water patch.
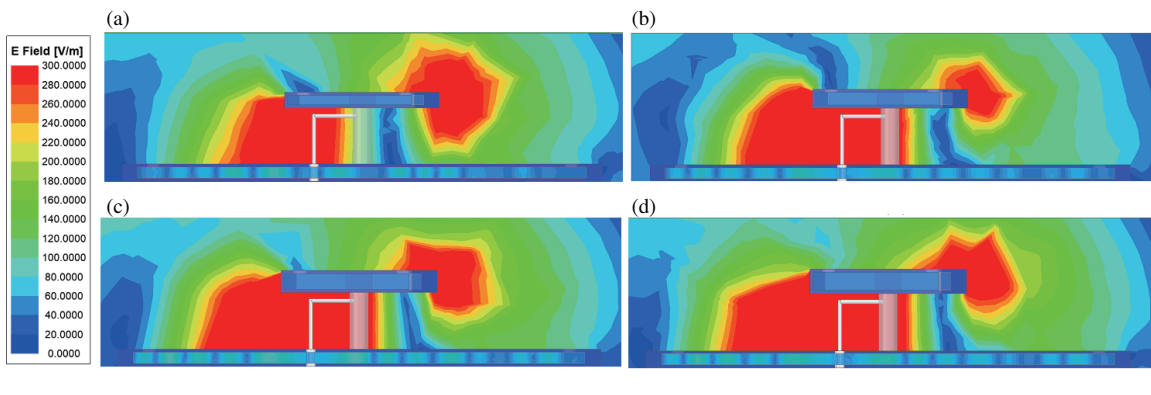
FIGURE 14. Electric field distributions of different water layer thicknesses on water patches (a) 3 mm. (b) 4 mm. (c) 5 mm. (d) 5.8 mm.

ter ground are the main sources of radiation, enlarging the area of these two slots by thickening the substrate allows more EM waves to radiate into free space, thus increasing the gain.

The performance parameters of antennas from other related literature are compared in Table 4. OT refers to optical transparency. BW refers to impedance bandwidth. The compari-

TABLE 4. Comparison between transparent antennas.

Ref.	Material	Probe-Feed	Reconfiguration	OT (%)	BW(%)	Efficiency (%)	Gain (dBi)
[6]	Distilled water	Polarization	L-shape probe	/	22	59	4.0
[8]	Distilled water	Frequency	No	/	23.9	85	7.2
[12]	TCO	No	No	90	44	83	6.2
[13]	TCF	No	coaxial probe	71	30.8	72.3	5.3
[14]	Mesh metal	No	coaxial probe	88	6.7	35	20.14
[16]	Distilled water	Frequency	Disk probe	/	40	80	3.8
[20]	Saltwater	No	No	60	14	34	1.91
[21]	Distilled water	No	No	100	15	68	5.5
This work	Distilled water	Frequency and Polarization	Γ-shaped probe	100	33	74.4	7.96
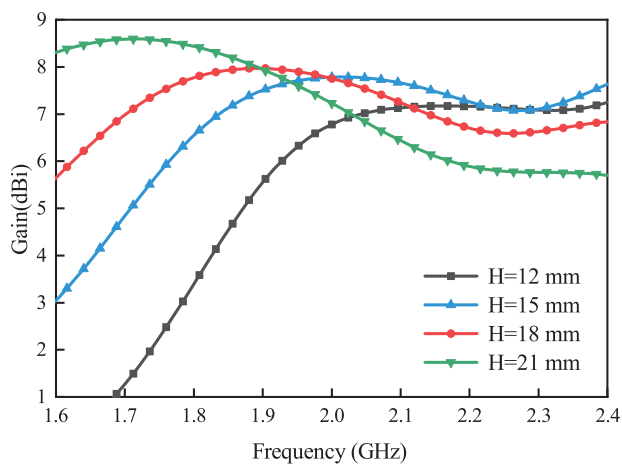
FIGURE 15. Simulated gain with different air substrate thicknesses.

son results show that the antenna has good gain and bandwidth in a fully transparent design while possessing both frequency and polarization reconfigurability. It also has the advantages of high optical transparency and low cost and offers a wide range of potential applications for transparent antennas.

6. CONCLUSION

In this paper, a transparent frequency and polarization reconfigurable water patch antenna is designed. The feasibility of using different liquid materials for transparent ground design is discussed, and the conclusions show that water is a better choice for transparent ground design. Both the patch and ground are composed of polyvinyl chloride material and distilled water to provide outstanding optical transparency at a minimal cost. Frequency and polarization reconfigurability were achieved by pumping distilled water into different cavities. In the field of transparent antenna applications, it will have an advantage over other transparent materials and can be applied to satellite communications. The antenna can also be used as a decoration in daily life. The transparent design reduces concerns about electromagnetic radiation when people see the antenna, and the water can be recycled as a liquid material, improving the environmental friendliness of the antenna.

REFERENCES

[1] Chen, Q., J. Ala-Laurinaho, A. Khripkov, J. Ilvonen, R. M. Moreno, and V. Viikari, "Varactor-based frequency-reconfigurable dual-polarized mm-Wave antenna array for mobile devices," *IEEE Transactions on Antennas and Propagation*, Vol. 71, No. 8, 6628–6638, 2023.

[2] Zainarry, S. N. M., S. J. Chen, and C. Fumeaux, "A frequency-reconfigurable single-feed zero-scanning antenna," *IEEE Transactions on Antennas and Propagation*, Vol. 71, No. 2, 1359–1368, 2022.

[3] Chen, Y., H. Guo, Y. Liu, J. Li, Y. Zhan, Q. Wu, and M. Li, "An L-slot frequency reconfigurable antenna based on MEMS technology," *Micromachines*, Vol. 14, No. 10, 1945, 2023.

[4] Nguyen, T. K., C. D. Bui, A. Narbudowicz, and N. Nguyen-Trong, "Frequency-reconfigurable antenna with wide-and narrowband modes for sub-6 GHz cognitive radio," *IEEE Antennas and Wireless Propagation Letters*, Vol. 22, No. 1, 64–68, 2022.

[5] Jin, X., S. Liu, Y. Yang, and Y. Zhou, "A frequency-reconfigurable planar slot antenna using S-PIN diode," *IEEE Antennas and Wireless Propagation Letters*, Vol. 21, No. 5, 1007–1011, 2022.

[6] Wang, M. and Q.-X. Chu, "A wideband polarization-reconfigurable water dielectric resonator antenna," *IEEE Antennas and Wireless Propagation Letters*, Vol. 18, No. 2, 402–406, 2019.

[7] Wang, F., W. Luo, Z. Xu, K. Li, and Y. Ren, "Directional high gain liquid antenna using tumbler-like dielectric resonator for wireless capsule endoscopes system," *IEEE Antennas and Wireless Propagation Letters*, Vol. 23, No. 11, 3709–3713, 2024.

[8] Chen, Z., H.-Z. Li, H. Wong, W. He, J. Ren, and T. Yuan, "A frequency-reconfigurable dielectric resonator antenna with a water layer," *IEEE Antennas and Wireless Propagation Letters*, Vol. 22, No. 6, 1456–1460, 2023.

[9] Wang, S., F. Fan, F. Zhang, Y. Li, G. Zhang, S.-W. Wong, and L. Zhu, "A frequency-reconfigurable inverted-L antenna made of pure water," *IEEE Antennas and Wireless Propagation Letters*, Vol. 21, No. 1, 109–113, 2021.

[10] Chen, Z., H.-Z. Li, H. Wong, X. Zhang, and T. Yuan, "A circularly-polarized-reconfigurable patch antenna with liquid dielectric," *IEEE Open Journal of Antennas and Propagation*, Vol. 2, 396–401, 2021.

[11] Li, L., X. Yan, H. C. Zhang, and Q. Wang, "Polarization-and frequency-reconfigurable patch antenna using gravity-controlled liquid metal," *IEEE Transactions on Circuits and Systems II: Express Briefs*, Vol. 69, No. 3, 1029–1033, 2022.

[12] Chishti, A. R., A. Aziz, M. A. Qureshi, M. N. Abbasi, A. M. Algarni, A. Zerguine, N. Hussain, and R. Hussain, "Optically transparent antennas: A review of the state-of-the-art, innovative solutions and future trends," *Applied Sciences*, Vol. 13, No. 1, 210, 2022.

[13] Montisci, G., G. Mura, G. Muntoni, G. A. Casula, F. P. Chietera, and M. Aburish-Hmidat, "A curved microstrip patch antenna designed from transparent conductive films," *IEEE Access*, Vol. 11, 839–848, 2022.

[14] Xi, B., X. Liang, Q. Chen, K. Wang, J. Geng, and R. Jin, "Optical transparent antenna array integrated with solar cell," *IEEE Antennas and Wireless Propagation Letters*, Vol. 19, No. 3, 457–461, 2020.

[15] Sun, J. and K.-M. Luk, "A wideband and optically transparent water patch antenna with broadside radiation pattern," *IEEE Antennas and Wireless Propagation Letters*, Vol. 19, No. 2, 341–345, 2019.

[16] Abdullah, A., S. I. H. Shah, S. Kiv, J. Ho, and S. Lim, "A low-cost microfluidic and optically transparent water antenna with frequency-tuning characteristics," *Micromachines*, Vol. 14, No. 11, 2052, 2023.

[17] Sun, J. and K.-M. Luk, "A wideband low cost and optically transparent water patch antenna with omnidirectional conical beam radiation patterns," *IEEE Transactions on Antennas and Propagation*, Vol. 65, No. 9, 4478–4485, 2017.

[18] Abdelbary, M. M., H. A. Malhat, and S. H. Zainud-Deen, "Circularly polarized reconfigurable water based microstrip antenna," in *2019 36th National Radio Science Conference (NRSC)*, 44–51, Port Said, Egypt, Apr. 2019.

[19] Stutzman, W. L. and G. A. Thiele, *Antenna Theory and Design*, John Wiley & Sons, 2012.

[20] Nguyen, T. D., J. H. Choi, and C. W. Jung, "Optically transparent patch antennas using saltwater for WLAN applications," *Journal of Electromagnetic Engineering & Science*, Vol. 22, No. 6, 609–615, 2022.

[21] Pijoan, J. L., S. Díaza, A. Andújar, and J. Anguera, "Water dielectric microstrip patch antenna: case study at ISM 2.4 GHz," *International Journal of Electronics*, Vol. 109, No. 3, 462–477, 2022.